HHS Public Access

Author manuscript

Opt Lett. Author manuscript; available in PMC 2019 September 06.

Published in final edited form as:

Opt Lett. 2015 April 01; 40(7): 1426–1429. doi:10.1364/OL.40.001426.

In Vivo Molecular Contrast OCT imaging of Methylene Blue

Wihan Kim, **Brian E. Applegate***

Department of Biomedical Engineering, 5045 Emerging Technology Building, 3120 Texas A&M University, College Station, TX 77843, USA

Abstract

An 830 nm spectral-domain Optical Coherence Tomography (OCT) system with an integrated 663 nm diode pump laser has been developed to enable molecular contrast OCT imaging of Methylene Blue (MB), a common vital dye used clinically. The introduction of the 663 nm diode laser, which acts as the pump in this implementation of Pump-Probe OCT (PPOCT), represents a minor modification to an otherwise typical OCT system. A newly developed background subtraction technique completely removes all background from intensity noise at the pump modulation frequency, simplifying the interpretation of PPOCT images. These developments have enabled the first *in vivo* imaging of MB with PPOCT. Volumetric images of a zebrafish, stained by submersion in a 0.01% (w/v) solution of MB for 6 hours, show accumulation of MB in the mesonephros, the primordial filtration organ.

Beyond the current clinical applications in ophthalmology and cardiology, Optical Coherence Tomography (OCT) is being widely investigated as a diagnostic and research tool for human disease and animal models of the same. It can provide non-invasive high-fidelity morphological images of highly scattering tissues at depths of 1–2 mm. The image contrast in OCT arises from variations in the tissue refractive index. Unfortunately in many cases there is very little change in the differential refractive index in morphologically distinct areas of soft tissues. One approach to engendering additional contrast is to use exogenous agents which are targeted either passively or actively to the morphological features of interest. Beyond simply highlighting a particular morphology this approach can target specific molecules or receptors to provide detailed information on the local biochemistry and yield enhanced visualization of pathological and physiological processes. This “molecular imaging” approach while common in microscopy is only slowly being adapted to OCT. A contributing factor is the lack of sensitivity to incoherent processes such as florescence emission and spontaneous Raman scattering.

Light absorption has been harnessed for contrast in several molecular imaging enabled OCT techniques. [1–4] In this letter, we will be interested in Pump-Probe OCT (PPOCT) [5] which measures transient absorption. The first contrast agent imaged with PPOCT was methylene blue (MB). [6] It has a well-known excited triplet state absorption centered around 830 nm. The triplet state is populated by pumping the singlet ground state into the first excited singlet state where strong spin-orbit coupling provides for efficient spontaneous

*Corresponding author: apple@tamu.edu.

intersystem crossing. This process is shown in the simplified energy level diagram in Figure 1(a). The ground state has a broad bandwidth absorption peaked at 660 nm. Excitation at 660 nm leads to transient absorption at 830 nm.

Methylene blue has a variety of clinical applications. It is a recommended treatment for methemoglobinemia [7]. Likewise it was one of the earliest antimalarial drugs [8]. It is also a common stain used in chromoendoscopy of the gastrointestinal tract.[9] In particular MB has been shown to selectively stain specialized columnar epithelium in Barrett's esophagus. [10] Monitoring of Barrett's esophagus is one of the emerging clinical applications of OCT technology. [11]

Prior efforts [5, 6] at imaging MB with PPOCT have utilized nanosecond pulsed lasers at 532 nm as the pump and femtosecond pulsed lasers at 830 nm as the probe. These succeeded in imaging tissue phantoms, however there has never been a demonstration in a biological sample, either *in vivo* or *ex vivo*. A contributing factor is the fairly weak absorption of the 532 nm light which is on the shoulder of the ground state absorption peak. A second issue with these studies is the use of fairly atypical OCT light sources. While femtosecond pulsed lasers have been demonstrated as sources for OCT many times, commercial instruments operating in the 800 nm band predominantly make use of superluminescent diodes which are far cheaper and more robust. Our goal for the work described here was to develop an approach which would enable imaging of MB at powers below the ANSI limits using more common and robust light sources. We were motivated by the fact that such a development would facilitate clinical translation of the technology.

As an initial step we took a fresh look at the choice of pump laser sources. Recognizing the inefficiency of the 532 nm excitation we looked to laser sources that could excite near the 660 nm peak where the absorption cross-section is a factor of 20 larger. Pulsed lasers with 10–100 kHz repetition rates at that wavelength are uncommon, hence we turned to continuous wave (cw) diode lasers that could be amplitude modulated. Such lasers are inexpensive, robust, and readily available. In this regime, where there is no longer short-pulse laser excitation, the timing between the pump and probe pulse is obviated, thus enabling the use of cw probes, such as a superluminescent diode. Since the probe is the OCT light source, this paradigm shift enabled PPOCT imaging of MB with only minor modifications to an 830 nm band spectral-domain OCT system.

The losses due to transient absorption can be modeled as a reduction in the sample reflectivity (R_s), where the OCT signal is proportional to $R_s^{1/2} = r_s$. In the case of absorption due the triplet state of MB the reflectivity becomes) $r_{s,0}(1 - \sigma_T N_T dz)$ where σ_T is the triplet state absorption cross-section, $N_T$is the triplet state population, dz is the pathlength, and we have assumed the weak absorption limit where the exponential function can be approximated by the first two terms of its Taylor series expansion. Prior to interacting with the pump laser, N_T is exactly zero. If we assume an impulse pump excitation, then N_T is populated by intersystem crossing from S_1 with a quantum efficiency of q and immediately begins to decay, yielding $N_T = qN_{S1}e^{-t/\tau}$ where τ^{-1} is the decay rate back to the ground state and the decay is assumed to be a single exponential. This approximation holds for short pulsed pump lasers as in our previous work. [5] There we were able to measure τ for MB by

varying the interpulse delay between the pump and probe to map out the decay and fit to a single exponential. In the case of a sine modulated pump laser $\left(\text{i.e. } \frac{P_{pu}}{2}[1+\sin\omega t]\right)$ we must explicitly consider the time dependent population of N_{S1}. Under these circumstances the triplet state population is proportional to the convolution, $N_T \propto [1 + \sin(\omega t)] \otimes e^{-t/\tau}$. Evaluating the convolution yields, $N_T \propto [1 + (1 + \omega^2\tau^2)^{-1/2}]$. where $\phi = \tan^{-1} \omega\tau$. Inserting a proportionality constant, β, to account for the efficiency with which the singlet excited (S_1) state is populated as well as folding in the quantum efficiency (q), the absorption cross-section (σ_T) and a factor of 0.5 we can rewrite the reflectivity as $r_s \approx r_{s,0}\,(1 - dzP_{pu}\beta[1 + (1 + \omega^2\tau^2)^{-1/2} \sin(\omega t - \phi)])$. Here we can see that the transient absorption signal will be sine modulated at the same frequency as the pump modulation with a phase shift of ϕ and scaled by $(1 + \omega^2\tau^2)^{-1/2}$. The phase shift and scaling are both dependent on the product of the modulation frequency and triplet state lifetime. This result is exactly analogous to frequency domain fluorescence lifetime microscopy where the phase of the signal is used to measure fluorescence lifetimes. [12] In our case the phase can be used to determine the triplet state lifetime.

The modified OCT system used for this study is shown schematically in Figure 1b. A superluminescent diode with ~40 nm bandwidth centered at 830 nm was used as the OCT light source. The pump source was a 663 nm diode laser (Toptica, iBeam Smart PT660) with a maximum output of 60 mW. The output of the diode laser could be sine modulated and/or pulsed. The 830 nm light was launched into a 2×2 fused fiber coupler that formed a Michelson interferometer. The 830 nm light in the sample arm also constitutes the probe. The pump beam was directed into the sample arm via a dichroic mirror. The pump and probe were focused at the same position to a spot diameter of ~19 μm and laterally scanned on the sample by a galvo mirror pair.. The signal due to the absorption of the pump was frequency encoded by modulation of the pump at 14 kHz in all cases. The detector was a custom spectrometer operated with a line rate of 40 kHz and 8 μs integration time. The spectral interferograms were processed in the typical way to generate OCT M-scans. The PPOCT signal was extracted from an M-scan via Fourier transform along the time axis and filtered as described previously [13].

Initially we conducted a simple experiment on a phantom to validate a new background subtraction method. The background arises from amplitude noise on the light source that decays approximately as 1/f. The phantom was a 200 μm inner diameter plastic capillary tube containing a flowing solution of 2% MB mixed with titanium oxide (Sigma-aldrich). The pump power was 4.4 mW and the probe was 1.4 mW. The tube was positioned at an angle to avoid the strong specular reflection from the tube surface. Figure 2a is the power spectrum at one depth in a PPOCT A-line of the phantom. The peak at 14 kHz (pump on) is the PPOCT signal. When the pump is off the PPOCT signal is gone, but the noise remains. As a result, there is a strong background signal which if left uncorrected could complicate the interpretation of PPOCT images. In order to mitigate this problem, we used a background normalization method to remove signal background due to source intensity noise at the pump modulation frequency. The background level at frequencies above and below (±2 kHz) the pump modulation frequency were measured and averaged. The implicit

assumption is that the background is well represented by a linear function over this small frequency range. The PPOCT signal was divided by the average noise background level, hence the mean of the noise background is 1. The normalized PPOCT signal was then thresholded to remove all of the noise background. We found that a threshold of 2.5 was sufficient to completely remove the background seen in the images of the phantom, Fig. 2b. This algorithm could be done on each pixel in the PPOCT image to enable essentially real-time measurement and removal of the background.

Using this same phantom we sought to estimate the sensitivity of the technique. The essential idea was to measure the signal as a function of concentration and extrapolate to a minimum measureable concentration. We can arrive at the appropriate relationship by recognizing that $r_{s,0}$ is measured directly by the conventional OCT signal and β is a linear function of the MB concentration (C). Since we only extract the sine modulated portion of r_s the ratio of the PPOCT/OCT signals is $dzP_{pu}\beta(1 + \omega^2\tau^2)^{-1/2}$ where other constants not specifically considered like detector responsivity cancel because they are the same in both the PPOCT and OCT signals. Since all other variables are known in a phantom experiment and only β varies with concentration, a measurement of this ratio as a function of concentration will reveal $\beta(C)$.

Measurements were made at 5 different concentrations of MB, 0.01%, 0.5%, 1%, 1.5% and 2%. The ratio $PPOCT/(OCTdzP_{pu})$ was calculated as a function of the concentration and the results fit to a line to get $\beta(\mu m^{-1}mW^{-1}) = 0.087C(w/v\%) + 8.7 \times 10^{-5}$ with an R^2 of 0.95. Based on these results, if we assume a pathlength of 15 μm, a pump power of 1 mW, a tissue reflectivity of −30 dB, and a system sensitivty of 110 dB we can expect to be able to measure 0.013% (41 μM) concentration of MB with a PPOCT SNR of 1 dB. Here we are not explicitly considering the attenuation of the pump beam. However, if we assume we started with the ANSI limit for skin at 660 nm (19 mW) at the tissue surface and assume the scattering coefficient of 10% intralipid is a reasonable approximation for tissue (56 cm^{-1} at 660 nm [14]), then the pump would be reduced to 1 mW of power at a depth of ~0.5 mm.

In order to exam the capacity to measure MB in a biological sample we chose to image larval stage zebrafish. Zebrafish are an important model for developmental biology as well as numerous human diseases. [15] Larval zebrafish, treated in accordance with an animal use protocol overseen by the Institutional Animal Care and Use Committee (IACUC) at Texas A & M University, were obtained 14 days after breeding. The zebrafish had been treated with PTU to suppress melanin expression and housed in water free of MB. In order to stain the embryos a 0.01% aqueous methylene blue solution was prepared. The embryo was transferred to the MB solution and remained there for 6 hours before imaging. For reference, aquarium water is frequently treated with a 10 times lower concentration of MB for its antiparasitic effect while for the identification of sentinel nodes [16] in breast cancer a solution about 100 times stronger is injected. The embryos were anesthetized with MS222 (250mg/L, tricaine) before imaging. For in vivo imaging the pump and probe had a power of 1.4 mW.

In order to verify where MB was accumulating in the treated zebrafish, we processed histological slides were prepared for both treated and untreated specimens, Fig. 3a and 3b,

respectively. The large dark areas on either side of the treated specimen near the midline correspond to the mesonephros, the basic excetory organ where MB is clearly accumulating in the treated sample. The mesonephros is the primodial kidney in fish and amphibians. MB is known to be cleared by the kidneys in humans when taken orally [17], so accumulation in the mesonephros was not unexpected. It is also rapidly reduced to leucomethylene blue which has no visible wavelength absorption and should be invisible to the PPOCT technique described here. It is likely that most of the MB was in the reduced form during the in vivo experiments and the intense blue coloring of the mesonephros is due to the fact that leucomethylene blue is also rapidly oxidized to MB by air [17] which would have happened during processing of the slides. In the untreated animal there are several dark areas at the top, bottom, and sides. It seems likely that these are due to incomplete suppression of melanin expression. The areas on the side coincide approximately to region of the mesonephros but are more superficial and likely due to highly pigmented stripes observed in adult zebrafish.

Just below the histology sections in Figure 3 (c, and d) are the fused OCT/PPOCT cross-sectional images generated by overlaying the background removed PPOCT image on top of the OCT image. The images are from a similar location, but different animals than the histology slides. PPOCT signal arises from the same region as the darkened areas in the histology slides. The size of stained region of the mesonophros also qualitatively agrees with the histology, showing a large stained area where the mesonephros should be. The PPOCT signal along the back and superficial along the midline of the fish are attributed to residual melanin.

Figure 3(e) is the fused OCT/PPOCT volume image. The 3-D volume clearly shows the depth of the PPOCT signal in the zebrafish where the mesonephros is stained. In addition to the PPOCT signal in the mesonephros, there is also signal in the eye. This could be due either to melanin in the retinal pigment epithelium or MB which is known to accumulate in the schlera in humans.

In conclusion, we have developed a PPOCT system architecture that requires only minor modification to a standard 830 nm OCT system but enables efficient detection of methylene blue. The limit of methylene blue detection (SNR=1dB) for a 15 μm thick sample at a depth of 0.5 mm, derived from phantom studies, is 41 μM.

Acknowledgement

This work was financially supported from the National Institutes of Health (NCRR, 1R21RR025799) and the National Science Foundation (CAREER, CBET-1055359).

References

1. Adler DC, Huang SW, Huber R, and Fujimoto JG, Optics Express 16, 4376–4393 (2008). [PubMed: 18542535]
2. Skala MC, Crow MJ, Wax A, and Izatt JA, Nano Letters 8, 3461–3467 (2008). [PubMed: 18767886]
3. Robles FE, Wilson C, Grant G, and Wax A, Nat Photonics 5, 744–747 (2011). [PubMed: 23144652]
4. Morgner U, Drexler W, Kartner FX, li XD, Pitris C, Ippen EP, and Fujimoto JG, Optics Letters 25, 111–113 (2000). [PubMed: 18059799]

5. Carrasco-Zevallos O, Shelton RL, Kim W, Pearson J, and Applegate BE, J Biophotonics (2013).
6. Rao KD, Choma MA, Yazdanfar S, Rollins AM, and Izatt JA, Optics Letters 28, 340–342 (2003). [PubMed: 12659437]
7. Wright RO, Lewander WJ, and Woolf AD, Annals of emergency medicine 34, 646–656 (1999). [PubMed: 10533013]
8. Schirmer RH, Coulibaly B, Stich A, Scheiwein M, Merkle H, Eubel J, Becker K, Becher H, Muller O, Zich T, Schiek W, and Kouyate B, Redox Rep 8, 272–275 (2003). [PubMed: 14962363]
9. Committee AT, Wong Kee Song LM, Adler DG, Chand B, Conway JD, Croffie JM, Disario JA, Mishkin DS, Shah RJ, Somogyi L, Tierney WM, and Petersen BT, Gastrointestinal endoscopy 66, 639–649 (2007). [PubMed: 17643437]
10. Canto MI, Setrakian S, Willis JE, Chak A, Petras RE, and Sivak MV, Endoscopy 33, 391–400 (2001). [PubMed: 11396755]
11. Suter MJ, Gora MJ, Lauwers GY, Arnason T, Sauk J, Gallagher KA, Kava L, Tan KM, Soomro AR, Gallagher TP, Gardecki JA, Bouma BE, Rosenberg M, Nishioka NS, and Tearney GJ, Gastrointestinal endoscopy (2014).
12. van Munster EB and Gadella TW, Advances in biochemical engineering/biotechnology 95, 143–175 (2005). [PubMed: 16080268]
13. Jacob D, Shelton RL, and Applegate BE, Optics Express 18, 12399–12410 (2010). [PubMed: 20588366]
14. Flock ST, Jacques SL, Wilson BC, Star WM, and van Gemert MJ, Lasers Surg Med 12, 510–519 (1992). [PubMed: 1406004]
15. Lieschke GJ and Currie PD, Nature reviews. Genetics 8, 353–367 (2007).
16. Golshan M and Nakhlis F, The breast journal 12, 428–430 (2006). [PubMed: 16958960]
17. DiSanto AR and Wagner JG, Journal of pharmaceutical sciences 61, 1086–1090 (1972). [PubMed: 5044807]

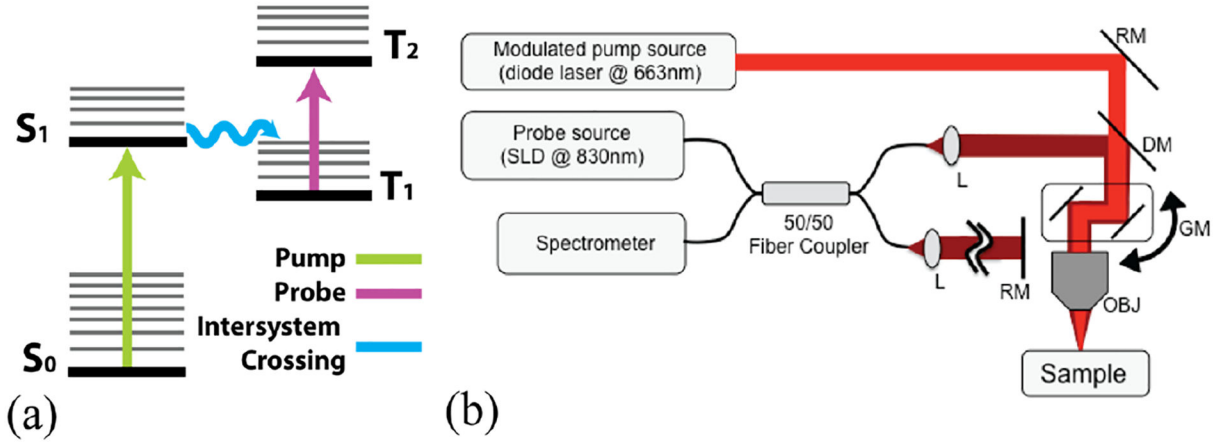

Fig. 1.

(a) Simplified energy level diagram for Methylene Blue. (b) PPOCT system schematic. Pump source: modulated 663nm diode laser, Probe source: SLD at 830 nm center wavelength, DM: dichroic mirror, RM: reference arm mirror, GM: galvanometer scanner, OBJ: objective lens.

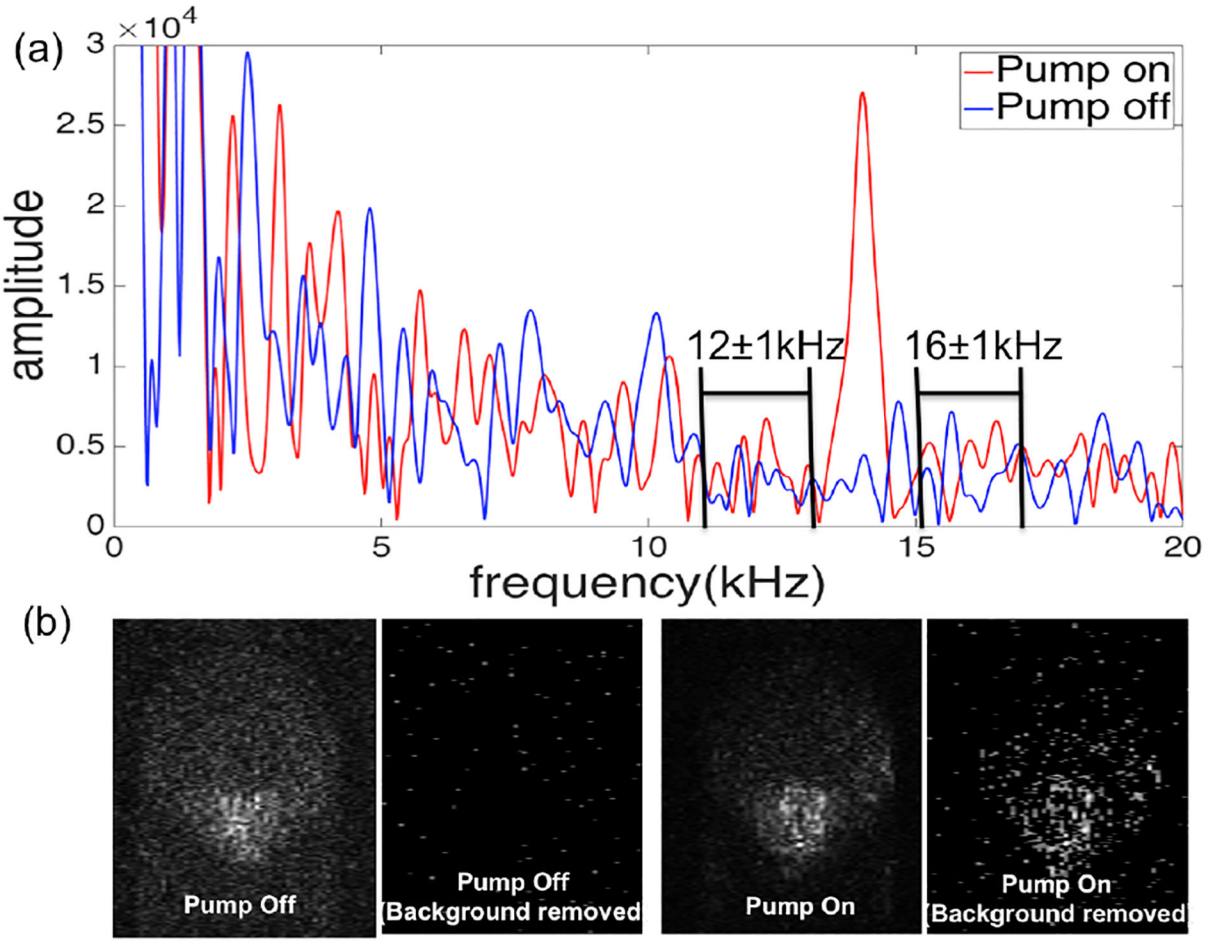

Fig. 2.

(a) Frequency domain signal from one pixel in the MB filled capillary tube with and without the pump on. The relevant aspects of the background subtraction algorithm are labeled where the background is assumed to vary linearly over a narrow frequency range. (b) comparison of PPOCT images with background subtraction demonstrating the complete removal of the of noise background.

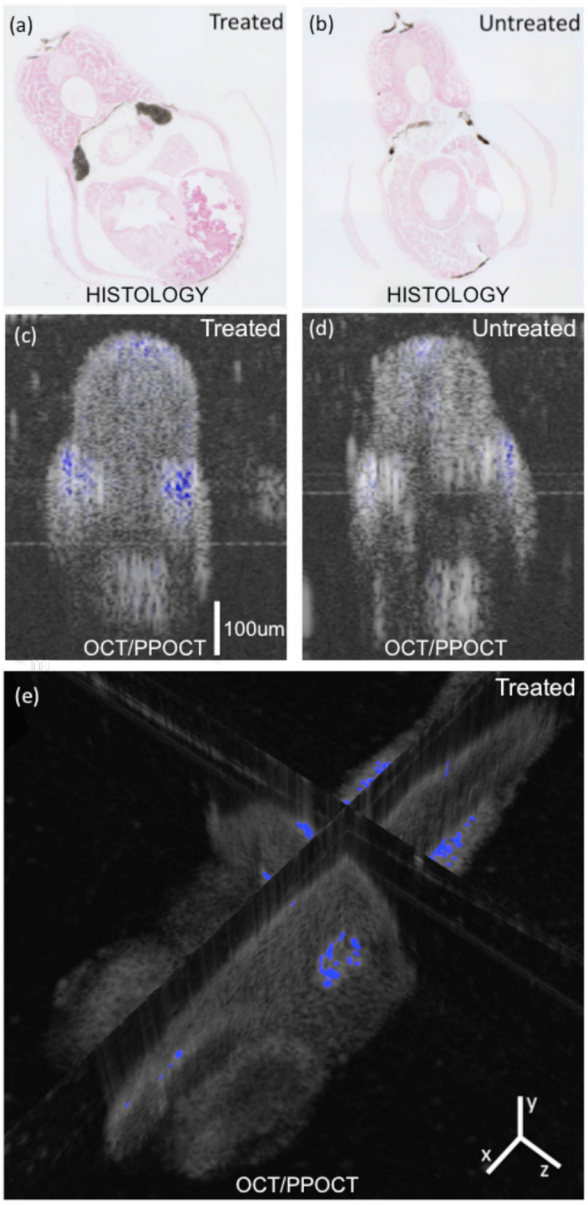

Fig. 3.

(a, b) Histological cross-section from a zebrafish. Treated corresponds to 0.01% (w/v) MB. Large dark areas at the midline of the treated animal are interpreted as accumulated MB in the mesonephros. Other dark areas also present in the untreated animal are attributed to residual melanin. (c, d) Corresponding PPOCT cross-sectional images. Note: OCT images shown on traditional log intensity scale and PPOCT shown on linear intensity scale. (e) Intersecting planes from volumetric data set with PPOCT signal and overlain on the OCT signal of a live zebrafish treated with MB.